

Degradation of GPS performance in geomagnetically disturbed conditions

E. L. Afraimovich, V. V. Demyanov, T. N. Kondakova

Institute of Solar-Terrestrial Physics SD RAS,

p. o. box 4026, Irkutsk, 664033, Russia

fax: +7 3952 462557; e-mail: afra@iszf.irk.ru

Short title: GPS PERFORMANCE DURING MAGNETIC STORMS

Abstract. The GPS performance is impaired in conditions of geomagnetic disturbances. The rms error of positioning accuracy increases in the case where two-frequency GPS receivers of three main types (Ashtech, Trimble, and AOA) are in operation. For Ashtech receivers (unlike AOA and Trimble) there is also a clear correlation between the slip density of the one- and two-frequency modes of positioning and the level of geomagnetic disturbance.

1. Introduction

The satellite navigation GPS system [*Hofmann-Wellenhof et al.*, 1992] has become a powerful factor of scientific and technological progress worldwide, and enjoys wide use in a great variety of human activity. In this connection, much attention is given to continuous perfection of the GPS system and to the widening of the scope of its application for solving the navigation problems themselves, as well as for developing higher-precision systems for time and accuracy determinations. Even greater capabilities are expected in the near future through the combined use of the GPS with a similar Russian system GLONASS [*Kharisov et al.*, 1998].

The performance of modern global satellite radio navigation systems that utilize the "Earth-Space" radio wave propagation channel is limited considerably by the influence of the geospace environment. Furthermore, the main contribution comes from systematic ionospheric effects of radio wave propagation: the group and phase delay, the frequency Doppler shift, and the rotation of the plane of polarization (Faraday effect). In many instances the degree of manifestation of the above effects has only a weak dependence on the local distribution of electronic density in the ionosphere but is directly correlated with the value of total electron content (TEC) along the radio signal propagation path [*Goodman and Aarons*, 1990].

In undisturbed geospace conditions the main contribution to the formation of the above-mentioned ionospheric effects is made by the regular TEC component. It undergoes periodic regular variations (seasonal-diurnal, latitudinal, and longitudinal) and is relatively accurately predictable. A variety of TEC models have been developed to date, which are intended to cancel out the ionospheric influence on the performance of the modern GLONASS and GPS in geomagnetically quiet and weakly disturbed conditions [*Afraimovich et al.*, 2000a; *Klobuchar*, 1986].

The situation with geomagnetically disturbed geospace is more complicated. The irregular TEC component makes a substantial contribution in this case. The amplitude of random TEC variations with a period from a few minutes to several hours in conditions of geomagnetic disturbances can make up as much as 50% of the background TEC value [*Basu et al.*, 1988; *Bhattacharrya et al.*, 2000; *Ho et al.*,

1996; *Shaer et al.*, 1997; *Warnart*, 1995]. Furthermore, the amplitude and phase fluctuation range of signals from navigation satellites (NS) at the reception point can exceed the designed level corresponding to the uninterrupted operation of GPS receivers. This leads to the degradation of the determination accuracy of a current location (CL) of stationary and mobile users of GPS. Furthermore, there might occur a break-down in tracking the NS signal in phase (code) one of the working frequencies and, hence, a failure in the determination of the coordinates in the one- or two-frequency mode.

The study of deep, fast variations in TEC caused by a strong scattering of satellite signals from intense small-scale irregularities of the ionospheric $F2$ -layer at equatorial and polar latitudes has a special place among ionospheric investigations based on using satellite (including GPS) signals [*Aarons*, 1982; *Basu et al.*, 1988; *Aarons et al.*, 1996, 1997; *Pi et al.*, 1997; *Aarons and Lin*, 1999].

Recent years saw extensive studies of phase fluctuations and phase slips of range measurements using GPS in conditions of geomagnetic disturbances [*Afraimovich et al.*, 2000; 2000a; 2001; 2001a; 2002; 2002a; *Bhattacharrya et al.*, 2000; *Skone and Jong*, 2000; *Coster et al.*, 2001; *Shan et al.*, 2002]. From the point of view of the GPS user, however, of significantly greater interest are the investigations into the influence of geomagnetic disturbances on the performance of GPS as a positioning system.

The objective of this paper is to estimate the CL determination accuracy and the failure density in determining the location in the one-frequency and two-frequency modes in conditions of geomagnetic disturbances for GPS receivers installed at permanent mid-latitude stations forming part of the global GPS network.

2. Experimental setup and data processing technique

In conducting the experiment in order to investigate the GPS performance in conditions of geomagnetic disturbances, we intended

- to estimate the CL determination accuracy of the GPS user in conditions of geomagnetic disturbances as compared to undisturbed conditions; and

- to establish the fact of presence (absence) of slips in the determination of the user's location in the one-frequency mode of standard accuracy and in the mode of two-frequency positioning in conditions of geomagnetic disturbances, and to obtain a numerical estimate of the slip density.

We used, as input experimental data, RINEX-files [Gurtner, 1993] available through the Internet at <http://lox.ucsd.cdu/cgi-bin/allCoords.cgi>. Of them, we considered the data from the set of stations forming part of the global GPS network (GPS stations) in the mid-latitude region (latitudes B - 35...50°, longitudes L -120...90°) in North America where the distribution density of stations is the largest (the location map of GPS stations is presented in Fig.1). We did not consider the equatorial and polar regions.

Three days were used in the experiment: one quiet day (July 12, 2000, day number in the year 194), and two magnetically disturbed days (July 15 and August 12, 2000, day numbers 197 and 225, respectively) when strong magnetic storms occurred.

It is pointed out in [Afraimovich *et al.*, 2000; 2000a; 2001; 2001a; 2002; 2002a] that geomagnetically disturbed conditions show a different response of two-frequency receivers manufactured by different firms. Thus, the lowest phase slip density of range measurements at the working frequencies f_1 and f_2 was observed for Ashtech receivers, a moderate density for Trimble, and the highest density for AOA. In this connection, our experiment was conducted with regards to GPS receivers of these types. Table 1 presents general information about the experiment: date; maximum level of geomagnetic disturbance characterized by the maximum value of the geomagnetic index $-Dst_{max}$, nT, for 24 hours; GPS station name and location, and the name of the receiver installed at a given station.

The goal of the first stage of GPS data processing in this paper is to reconstruct the current location on the basis of available RINEX files using software product TEQC posted by its developers on the Internet at: <http://unavco.ucav.edu/data-support/software/teqs/tewc.html> which we updated to ease the experiment.

In order to carry out investigations into the above-mentioned issues, we

developed software package "Navigator" to perform the following functions:

- automated start of software product TECQ in the package mode by setting up a current command line of the form: $teqc.exe + qc = stYYmmddhh/MMSS + dh\Delta t - navsitesddd0.YYnsitesddd0.YY o$, where $teqc.exe$ is the executed file of software product TECQ; qc , st , and dh are the control options in the command line; YY , mm , dd , MM , and SS are the year, month, day, hour, minute, and second for which the coordinates of the object are calculated with a current start of TECQ; Δt is the time step of calculation of the coordinates on the interval of observation (in fractions of an hour); and $sites$ is the abridged name of the GPS station, to which the RINEX-files of format "o" (observation) and "n" (navigation) refer.

- setting up of the output data file in the format:

$t_i; X_i; Y_i; Z_i; L_i; B_i; H_i; \Delta X_i; \Delta Y_i; \Delta Z_i; \Delta L_i; \Delta B_i; \Delta H_i$, where t_i is a current time (in hours and in fractions of an hour); X_i, Y_i , and Z_i are current rectangular geocentric coordinates (in meters); L_i, B_i , and H_i are current geocentric coordinates; and $\Delta X_i; \Delta Y_i; \Delta Z_i; \Delta L_i; \Delta B_i; \Delta H_i$ are absolute current errors of determination of the corresponding rectangular and geocentric coordinates.

- detecting the slips of the one- and two-frequency mode of positioning, and determining the corresponding slip density;

- estimating the current and daily mean spherical standard deviations of CL determination for the GPS station.

The software package is controlled through the interactive file in which the following data are specified:

- name of GPS station sites; - form of the command line (if necessary, the form of the command line can be changed); - date (day, month, day); - start and end time of the period of observation (in hours, minutes and seconds); - size of the time step of calculation of the current coordinates (Δt : from 0.018 to 24 hours); - direction of count time increment – toward increasing ($+dh$) or decreasing ($-dh$), respectively; - ON- (OFF-) option of the block of analyzing the slip density and the stands deviations of CL determination.

As a result of the first stage of processing, for each GPS station from Table 1 we

reconstructed for three days (194, 197, and 225) of the year 2000 the diurnal series of rectangular geocentric coordinates $X_i; Y_i; Z_i$; at time steps of 1.2 minute (the minimum possible steps when using the TEQC package), and the corresponding absolute errors:

$$\Delta x = x_i - x_0; \Delta y = y_i - y_0; \Delta z = z_i - z_0,$$

where x_0, y_0, z_0 are the known coordinates of the GPS station, and i is the time count number.

The second stage of data processing involved estimating the current CL determination accuracy that is equal to the value of the spherical standard deviation (SD) in the determination of the coordinates $\sigma(t_i)$, m:

$$\sigma(t_i) = (\sigma_{xi} + \sigma_{yi} + \sigma_{zi})^{0.5},$$

where $\sigma_{xi}, \sigma_{yi}, \sigma_{zi}$ are the SD in the determination of the corresponding coordinate in a rectangular geocentric coordinate system. Current values of $\sigma(t_i)$ were calculated for each 3.6-minute interval over the length of the entire diurnal series.

In addition, for a generalized estimation of the determination accuracy of the coordinate of each station in particular geomagnetic conditions, we calculated the daily mean values of the spherical SD $\bar{\sigma}$, m. Results of this processing are plotted as $\sigma(t)$ in Figs.2,3,4,5,6,7 are presented as histograms for $\bar{\sigma}$ (Fig.8).

The third stage of data processing included estimating the slip density in the determination of the CL for receivers of three types (Ashtech, AOA, and Trimble) in the one- and two-frequency modes. In the analysis of the slip intensity in the determination of the coordinates in the one-frequency mode, the slip was considered to mean the event implying that the following condition is satisfied:

$$\sigma(t) \leq \Pi = 500 \text{ m}$$

We deduced empirically the value of the unacceptable error threshold $\Pi = 500$ m, based on the fact that the best determination accuracy of CL is required for most practical purposes [Skone and Jong, 2000].

By the slip in the mode of two-frequency determination of the coordinates was meant the event implying that at a current instant of time, more than 30% of all observed NS of the constellation do not provide tracking at the auxiliary working

frequency f_2 .

As the characteristic of the slip intensity of the one- and two-frequency mode of coordinate determination, we calculated the current slip densities of the one- and two-frequency modes (N_1 and $N_{1,2}$, respectively). The current slip density N_1 and $N_{1,2}$ was determined as the total number of slips on each 0.5-hour interval. Results of this processing are presented as plots of the diurnal slip density distribution for the one-frequency mode (Fig.10,11,12), and for the two-frequency mode (Fig.13,14,15).

Furthermore, we also determined the total diurnal slip density N_s for the one- and two-frequency modes, for each station and for each of the days listed in Table 1. Results of this processing are represented by the histograms in Figs.9 and 16, respectively.

3. Results and discussion

3.1. The magnetically quiet day of July 12, 2000

Fig.2 (panels b,c,d) and Fig.3 (b,c) plot the time dependencies of the spherical standard deviations $\sigma(t)$ in the CL determination on the magnetically quiet day of July 12, 2000, obtained at three different sites: Kew1, Stb1, and Chb1 with the Ashtech receivers, and at sites Ursa (Trimble) and Algo (AOA). Table 2 presents the corresponding daily mean values of $\bar{\sigma}$. On some of the panels where the maximum values of standard deviations far exceeded the daily mean values, these values of the maximum diurnal standard deviation σ_{max} are included in Table 2 and removed from the figures to ease the reading. A more general picture of the daily mean values of standard deviations for all types of receivers for the days analyzed in this paper is provided by the Fig.8 histograms. In this figure, each type of receiver under investigation is represented by a set of three stations. Ashtech is represented on panel a) by the sites Kew1, Stb1, and Chb1; AOA is represented on panel b) by the sites Algo, Gode, and Usno; and Trimble is represented on panel c) by the sites Tung, Dyer, and Ursa.

It is evident from the figures and histograms presented here that in magnetically quiet conditions the CL determination accuracy that is provided by the Ashtech

and AOA receivers differs only slightly (for Ashtech $\bar{\sigma} \leq 46$ m, and for AOA $\bar{\sigma} \leq 33$ m). Single abrupt changes of the current values of $\sigma(t_i)$ over the course of 24 hours occur for the three types of receivers (Table 2). Furthermore, their maximum values do not differ greatly $\sigma_{max} \leq 249$ m for Ashtech; $\sigma_{max} \leq 256$ m for AOA, and $\sigma_{max} \leq 243$ m for Trimble.

As regards the number of slips in the coordinate determination in the one-frequency mode under quiet geomagnetic conditions, and Ashtech and AOA receivers also showed about the same level. Thus, no more than three slips of the one-frequency mode and no more than two slips were observed for 24 hours, respectively for Ashtech (site Kew1) and AOA (site Gode). For the Trimble receiver, this figure was worse and reached ten slips for 24 hours (site Tung). On the other hand, the three types of receivers at some of the sites did not show any slips of the one-frequency mode for 24 hours (see Fig.9). All observed slips occurred before 12 UT.

The performance of the Trimble receivers in the two-frequency mode of coordinate determination in the magnetically quiet situation was also worse when compared with Ashtech and AOA. Thus, for the receivers of the two last types, no slip of the two-frequency mode was recorded for all the sites under consideration (see Fig.13).

3.2. The magnetic storms of July 15 and August 12, 2000

In general, the period of geomagnetic disturbances showed a degradation of the accuracy and quality of GPS performance for the three types of receivers.

During the July 15 magnetic storm there was an increase of the value of the daily mean spherical standard deviation in the CL determination $\bar{\sigma}$, m. The corresponding maximum values were as follows: 76 m for the Ashtech receiver (site Kew1); 39 m for AOA (site Algo), and 120 m for Trimble (site Upsa). Thus the value of $\bar{\sigma}$ increased (compared to geomagnetically quiet conditions) by a factor of 1.6-1.7 for Ashtech, and by a factor of 1.1-1.2 for AOA and Trimble (for the sites Algo and Upsa, respectively). The estimates made here and Figs.3,6 and 8 suggest also the conclusion that the Ashtech receivers were the most sensitive to a change

of the geomagnetic situation. Values of the spherical SD in the CL determination using the AOA and Trimble receivers do not increase as significantly as above and can, in some cases, also be lower than those in geomagnetically quiet conditions (Fig.8 (a-c)).

A similar picture is also observed during the magnetic storm of August 12, 2000; however, the effect is more fully manifested. There was an unambiguous increase of the values of $\bar{\sigma}$ for the three types of receivers and for all sites when compared with magnetically quiet conditions. Values of $\bar{\sigma}$ increased by a factor of 1.6-2.6, 1.3-2.1 and 1.02-1.4 for Ashtech, AOA and Trimble (Fig.4 (b, c, d); 7 (b, c), and 8).

Table 2 presents the maximum values of single abrupt changes of current values of the spherical SD in the CL determination $\sigma(t_i)$ for the 24 hours that are analyzed. For the Ashtech and Trimble receivers, there is also a consistent tendency of the values of these abrupt changes to increase in geomagnetically disturbed conditions. Figs.3 (b, c); 4 (b, c, d) induce us also to suggest that for Ashtech the intervals with the largest number of abrupt changes of current values of $\sigma(t_i)$ correspond to the time period of the highest level of geomagnetic field disturbance. However, to confirm this assumption requires an extensive set of observations.

On the basis of studying the slip density and localization of the one- and two-frequency modes in the CL determination, the following features were established.

Firstly, we identified an unambiguous tendency of the slip density of the one-frequency mode to increase in magnetic storm conditions for the Ashtech and Trimble receivers. Compared to magnetically quiet conditions, the slip density of the one-frequency mode increased by a factor of 2.5 and 1.4-8 for Ashtech and Trimble, respectively (Fig.9, Figs.10 (b, d); 11 (b, d); 12 (b, d)).

Secondly, for the Ashtech receiver the localization of slips of the one-frequency mode along the time axis corresponds to the time period of maximum geomagnetic field disturbance (Figs.11b; 12b). The sole exception was the Ashtech receiver at the site Chb1. No slips of the one-frequency mode was recorded for this site for any one of the days under consideration.

Thirdly, we detected a clearly pronounced tendency of the slip density of the two-frequency mode in the CL determination to increase for the Ashtech receivers in geomagnetically disturbed conditions. Thus, while no slips were observed for the magnetically quiet day of July 12, at periods of geomagnetic disturbances their diurnal number varied from 40 (site Stb1, August 12) to 120 (site Kew1, July 15) – Fig.16.

Besides, there was a clear localization of the two-frequency mode for the time interval corresponding to the maximum level of geomagnetic field disturbance (Figs.14 (a, b) and 15 (a, b)). A similar, but less clearly pronounced, tendency of the slip density of the two-frequency mode to increase was also identified for the Trimble receivers (Fig.16b). We recorded no slips of the two-frequency mode in magnetic storm conditions for the AOA receivers in all cases that were considered.

Thus our investigation has shown that geomagnetic disturbances of geospace are accompanied by a degradation of the accuracy and quality of GPS performance. During geomagnetic disturbances of geospace the Earth's ionosphere becomes essentially inhomogeneous. The dramatic irregular geospace variations during geomagnetic disturbances are associated with the generation in the ionosphere of a broad spectrum of irregularities giving rise to the scattering and defocusing of the satellite signal.

As a result, receivers can observe significant signal amplitude fluctuations capable of causing the break-down of its tracking. Besides, the presence of irregular electron density irregularities along the radio signal propagation path is responsible for the proportionate fluctuations of the group and phase delay [Yakovlev, 1996] which degrade the accuracy of CL determination. Abrupt fluctuations of the phase delay can also cause the breakdown of NS signal tracking if the frequency Doppler shift of the received signal exceeds the frequency bandwidth of the tracking contour in phase.

As has been shown above, slips of the two-frequency mode of coordinate determination are a more common phenomenon compared with slips of the one-frequency mode. The main reason for this might be the fact that the signal level at the auxiliary (closed) frequency f_2 is lower than that at the fundamental

frequency f_1 . The received power, with the elevation angle of the ray to the NS of 45° , is 159 Db/W at the frequency f_1 , and 166 Db/W at the closed frequency f_2 [*Interface Control Document*; Langley, 1998]. As far as the differences between the response of the particular types of GPS receivers to geomagnetic disturbances of geospace are concerned, this issue still remains open and is beyond the scope of this paper. To elaborate on this question requires analyzing the design and functional features of receivers manufactured by different firms.

4. Conclusion

Main results of this study are as follows:

1. In geomagnetically disturbed conditions of geospace the accuracy and quality of GPS performance is impaired.
2. Unlike geomagnetically quiet conditions, the magnetic storm conditions are accompanied by an increase of the spherical standard deviation in the location determination for all types of GPS receivers. Furthermore, there was a maximum increase of the values of $\bar{\sigma}$ by a factor of 2.6, 2.1 and 1.4 for the Ashtech, AOA and Trimble receivers, respectively.
3. In magnetic storm conditions there is an increase of the number of slips of the one-frequency mode of coordinate determination. The slip density increased by a factor of 2.5, 8 and 12 for the Ashtech, Trimble and AOA receivers, respectively (site Usno).
4. We have identified an unambiguous tendency of the slip density of the one-frequency mode to increase for the Ashtech and Trimble GPS receivers, respectively. For the AOA receivers this tendency was observed not in all cases that were considered.
5. The slip density in the two-frequency mode of coordinate determination in magnetic storm conditions increases most dramatically for the Ashtech receivers (from 0 to 120 slips). As regards the Trimble receivers, there is a similar, but less clearly pronounced, picture (the slip density increased by a

factor of 1.5-2, on average). No slips of the two-frequency mode was detected for the AOA receivers in the cases under consideration.

Acknowledgments. The authors are grateful to G. V. Popov and V. G. Eselevich for their encouraging interest in this study and active participation in discussions. The authors are also indebted to E. A. Kosogorov and O. S. Lesuta for preparing the input data. Thanks are also due V. G. Mikhalkovsky for his assistance in preparing the English version of the \TeX manuscript. This work was done with support from the Russian Foundation for Basic Research (grants 01-05-65374 and 00-05-72026) and from RFBR grant of leading scientific schools of the Russian Federation 00-15-98509.

References

- Aarons, J.**, Global morphology of ionospheric scintillations. *Proceedings of the IEEE*, **70(4)**, 360–378, 1982.
- Aarons, J., Mendillo, M., Kudeki, E., and Yantosca, R.**, GPS phase fluctuations in the equatorial region during the MISETA 1994 campaign, *J. Geophys. Res.*, **101**, 26851–26862, 1996.
- Aarons, J., Mendillo, M., and Yantosca, R.**, GPS phase fluctuations in the equatorial region during sunspot minimum, *Radio Science*, **32**, 1535–1550, 1997.
- Aarons, J., and Lin, B.**, Development of high latitude phase fluctuations during the January 10, April 10-11, and May 15, 1997 magnetic storms, *J. Atmos. Terr. Phys.*, **61**, 309–327, 1999.
- Afraimovich, E.L., Lesyuta, O.S., Ushakov, I.I.**, Magnetospheric disturbances, and the GPS operation, *LANL e-print archive*, 2000, <http://xxx.lanl.gov/abs/physics/0009027>.
- Afraimovich, E.L., Chernukhov, V.V., Demyanov, V.V.**, Updating the ionospheric delay model for single-frequency equipment of users of the GPS, *Radio Science*, **35**, N1, 257–262, 2000a.
- Afraimovich, E.L., Berngardt, O.I., Lesyuta, O.S., Potekhin, A.P., and Shpynev, B.G.**, A Case Study of The Mid-Latitude GPS Performance at Nighttime During The Magnetic Storm of July 15, 2000. *Proceedings of International Beacon Satellite Symposium, June 4-6, 2001, Boston College, Institute for Scientific Research, Chestnut Hill, MA, USA*, 408–412, 2001.
- Afraimovich, E.L., Lesyuta, O.S., and Voeykov, S.V.**, GPS phase slips on L1-L2 and L1 frequencies during geomagnetic disturbances *Proceedings of International Beacon Satellite Symposium, June 4-6, 2001, Boston College, Institute for Scientific Research, Chestnut Hill, MA, USA*, 191–195, 2001a.
- Afraimovich, E.L., Lesyuta, O.S., and Ushakov, I.I.**, Geomagnetic disturbances, and the GPS operation, *Geomagnetism and Aeronomy*, **42**, N2, 220–227, 2002.
- Afraimovich, E.L., Lesyuta, O.S., Ushakov, I.I., and Voeykov, S.V.**, Geomagnetic storms and the occurrence of phase slips in the reception of GPS signals, *Annals of Geophysics*, **45**, N 1, 55–71, 2002a.

- Basu Santimay, MacKenzie E., and Basu Sunanda**, Ionospheric constraints on VHF/HUF communications links during solar maximum and minimum periods, *Radio Science*, **23**, 363–378, 1988.
- Bhattacharrya, A., Beach, T. L., Basu, S., and Kintner, P. M.**, Nighttime equatorial ionosphere: GPS scintillations and differential carrier phase fluctuations, *Radio Science*, **35**, 209–224, 2000.
- Coster, A.J., Foster, J.C., Erickson, P.J., Rich, F.J.**, Regional GPS Mapping of Storm Enhanced Density During the July 15-16 2000 Geomagnetic Storm, *Proceedings of International Beacon Satellite Symposium, June 4-6, 2001, Boston College, Institute for Scientific Research, Chestnut Hill, MA, USA*, 176–180, 2001.
- Goodman, Dj. M., Aarons, J.**, Ionospheric Effects on Modern Electronic System, *Proceedings of the IEEE*, **78**, N.3, 512–528, 1990.
- Gurtner, W.**, RINEX: The Receiver Independent Exchange Format Version 2, <http://igscb.jpl.nasa.gov/igscb/data/format/rinex2.txt>, 1993.
- Ho, C.M., Mannucci, A.J., Linqwister, U. J. et al.**, Global ionosphere perturbations monitored by the worldwide GPS network, *Geophys. Res. Letters*, **23**, N 22, 3219–2222, 1996.
- Hofmann-Wellenhof, B., Lichtenegger, H. and Collins, J.**, Global Positioning System: Theory and Practice. *Springer-Verlag, New York*, 1992, p. 327.
- Interface Control Document, ICD-200c; <http://www.navcen.uscg.mil/pubs/gps/icd200/>.
- Kharisov, V. N., Perov, A. I., and Boldin, V. A.**, The Global Satellite Radio Navigation GLONASS System. IPRZhR, Moscow, 1998, p. 509 (in Russian).
- Klobuchar, J.**, Ionospheric time-delay algorithm for single-frequency GPS users, *IEEE Transactions on Aerospace and Electronics System*, 1986. *AES*, **23(3)**, 325–331, 1986.
- Langley, R. B.**, GPS for Geodesy, Springer – Berlin, Heidelberg, New York, Barcelona, Budapest, Hong Kong, London, Milan, Paris, Singapore, Tokyo, 111–149, 1998.
- Pi, X., Mannucci, A. J., Lindgwister, U. J., and Ho, C. M.**, Monitoring of global ionospheric irregularities using the worldwide GPS network, *Geophys. Res. Lett.*, **24**, 2283–2286, 1997.

- Shaer et al.**, Global and Regional Ionospheric model using GPS double difference phase observable, *IGS worksh. Proc.*, 77–91, 1997.
- Shan, S.J., Lin, J.Y., Kuo, F.S. et al.**, GPS phase fluctuation observed along the American sector during low irregularity activity months of 1997-2000, *Earth, Planets and Space*, **54**, N2, 141–152, 2002.
- Skone, S., and de Jong, M.**, The impact of geomagnetic substorms on GPS receiver performance, *Earth, Planets and Space*, **52**, 1067–1071, 2000.
- Warnart, R.**, The study of the TEC and its irregularities using a regional network of GPS stations, *IGS worksh. Proc.*, 249–263, 1995.
- Yakovlev, O. I.**, Cosmic radiophysics. *Moscow: Nauka*, 1996, p. 432.

E. L. Afraimovich, V. V. Demyanov, T. N. Kondakova, Institute of Solar-Terrestrial Physics SD RAS, p. o. box 4026, Irkutsk, 664033, Russia, fax: +7 3952 462557; e-mail: afra@iszf.irk.ru

Received _____

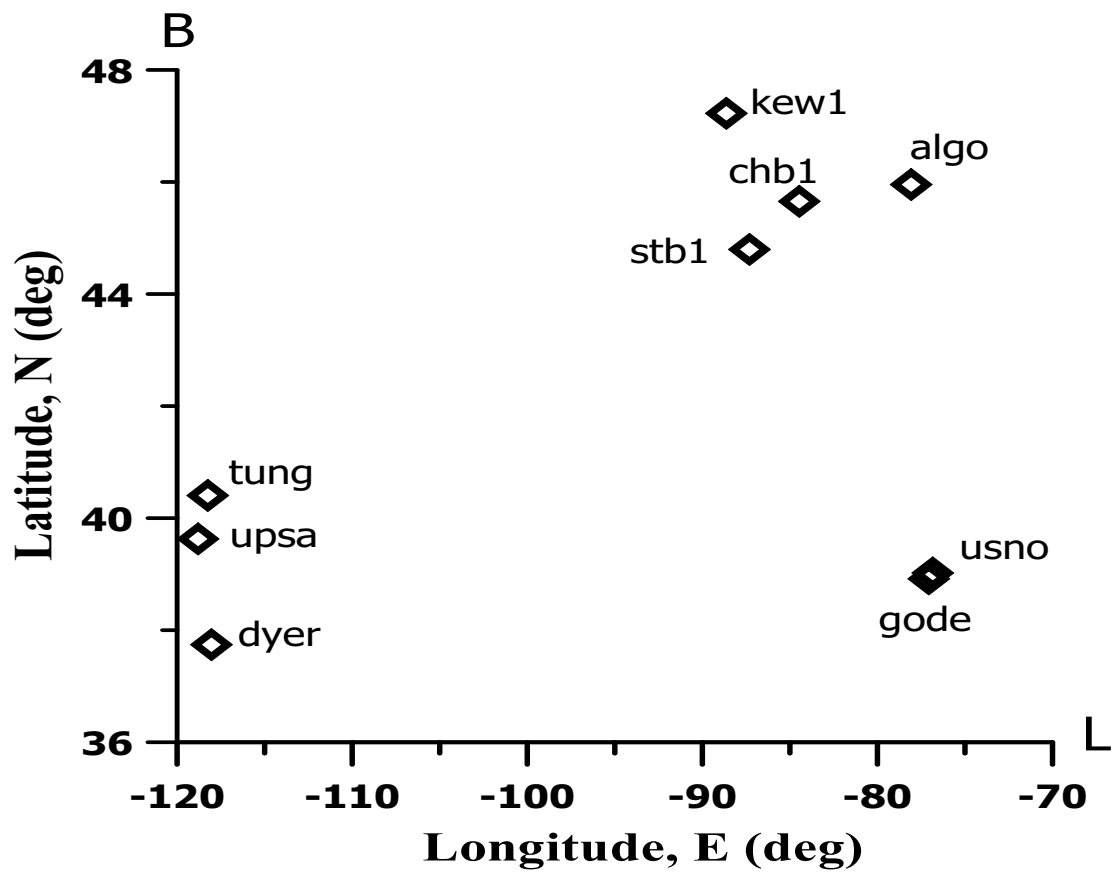


Figure 1: The map showing the locations of the receiving stations of the global GPS system. The number of receiving sites totals no less than 1000 as of the beginning of 2002.

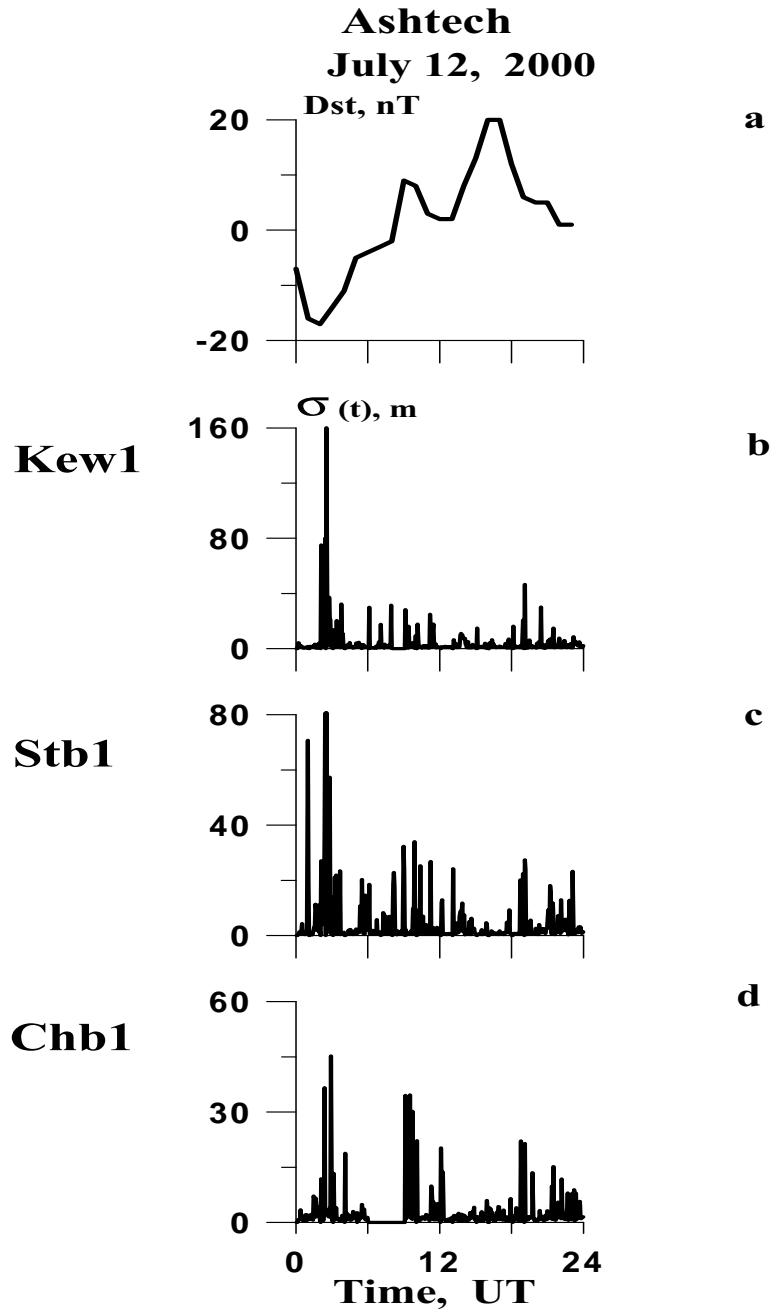


Figure 2: Diurnal variations of the magnetic disturbance index Dst for the magnetically quiet day of July 12, 2000 - panel a). Diurnal variations of the standard deviation $\sigma(t), m$ in the location determination, inferred using the data from the Ashtech receivers installed at Kew1 - b), Stb1 - c), and Chb1 - d).

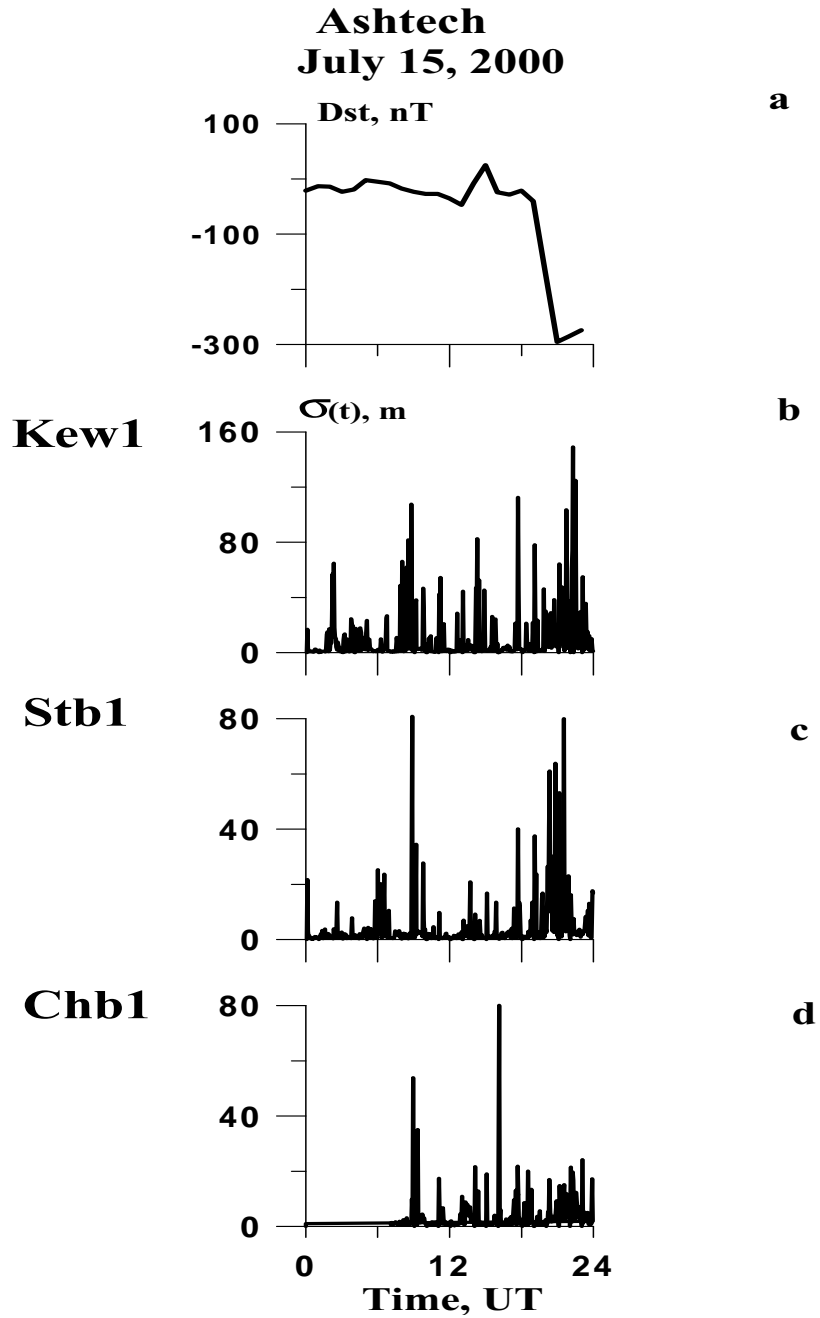


Figure 3: Diurnal variations of the magnetic disturbance index Dst for the magnetically disturbed day of July 15, 2000 - panel a). Diurnal variations of the standard deviation $\sigma(t)$, m in the location determination, inferred using the data from the Ashtech receivers installed at Kew1 - b), Stb1 - c), and Chb1 - d).

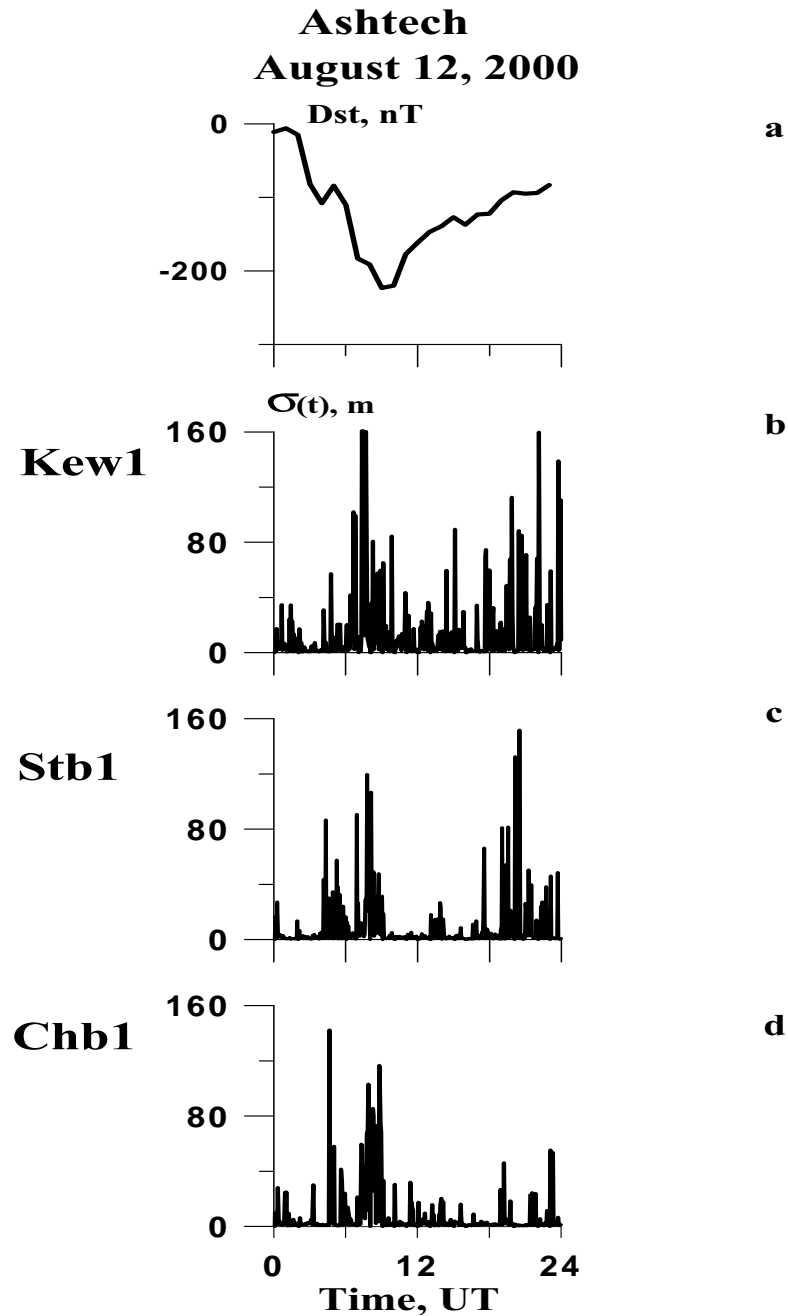


Figure 4: Diurnal variations of the magnetic disturbance index Dst for the magnetically disturbed day of August 12, 2000 - panel a). Diurnal variations of the standard deviation $\sigma(t), m$ in the location determination, inferred using the data from the Ashtech receivers installed at Kew1 - b), Stb1 - c), and Chb1 - d).

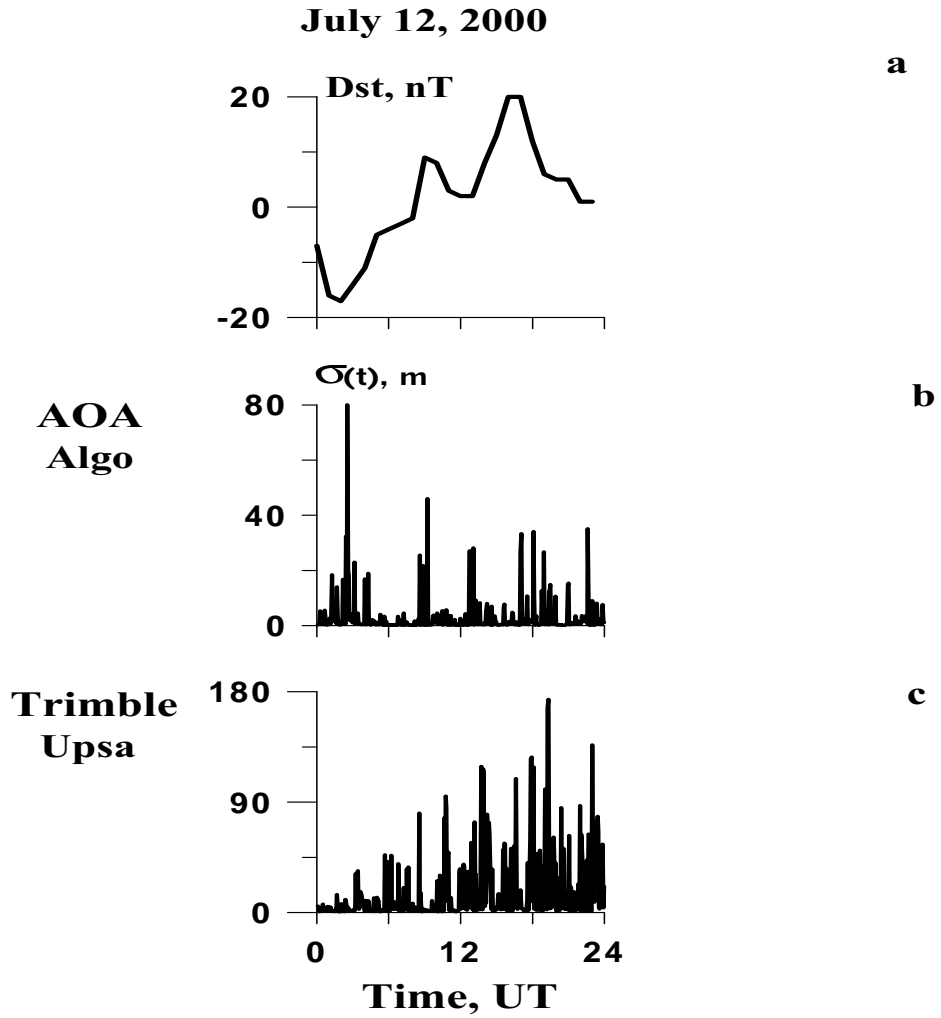


Figure 5: Diurnal variations of the magnetic disturbance index Dst for the magnetically quiet day of July 12, 2000 - panel a). Diurnal variations of the standard deviation $\sigma(t), m$ in the location determination, inferred using the data from the AOA receiver installed at Algo - b) and from the Trimble receiver installed at Upsa - c).

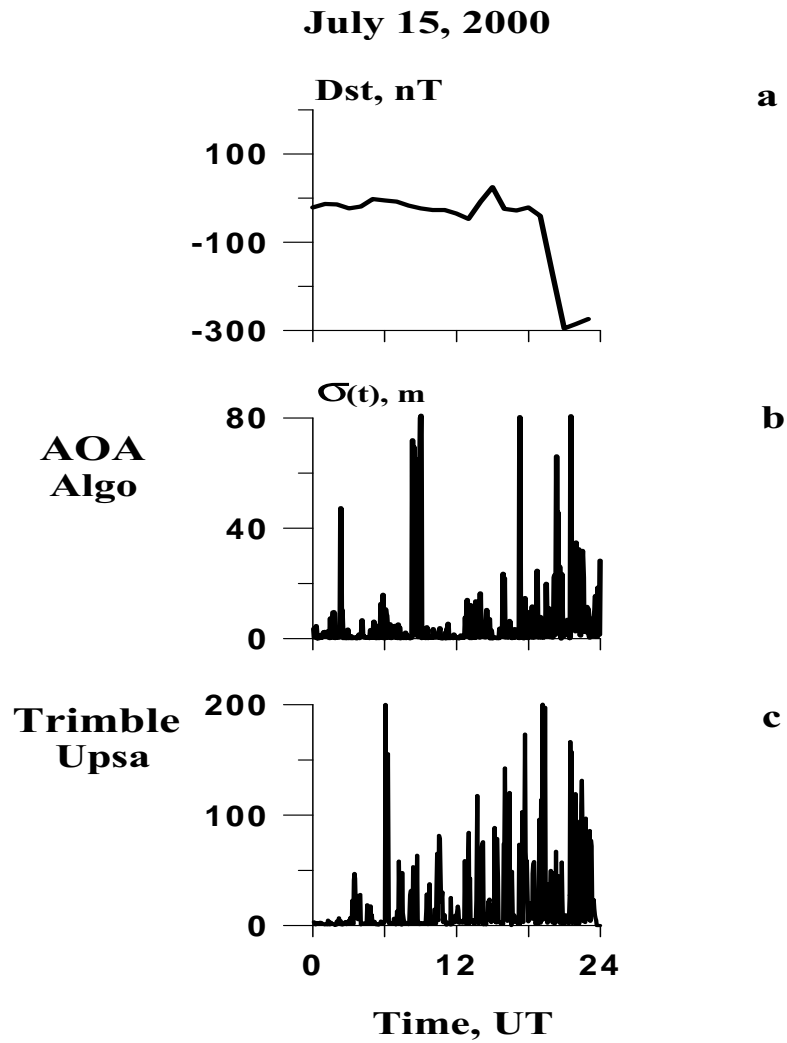


Figure 6: Diurnal variations of the magnetic disturbance index Dst for the magnetically disturbed day of July 15, 2000 - panel a). Diurnal variations of the standard deviation $\sigma(t)$, m in the location determination, inferred using the data from the AOA receiver installed at site Algo - b) and data from the Trimble receiver installed at site Upsa - c).

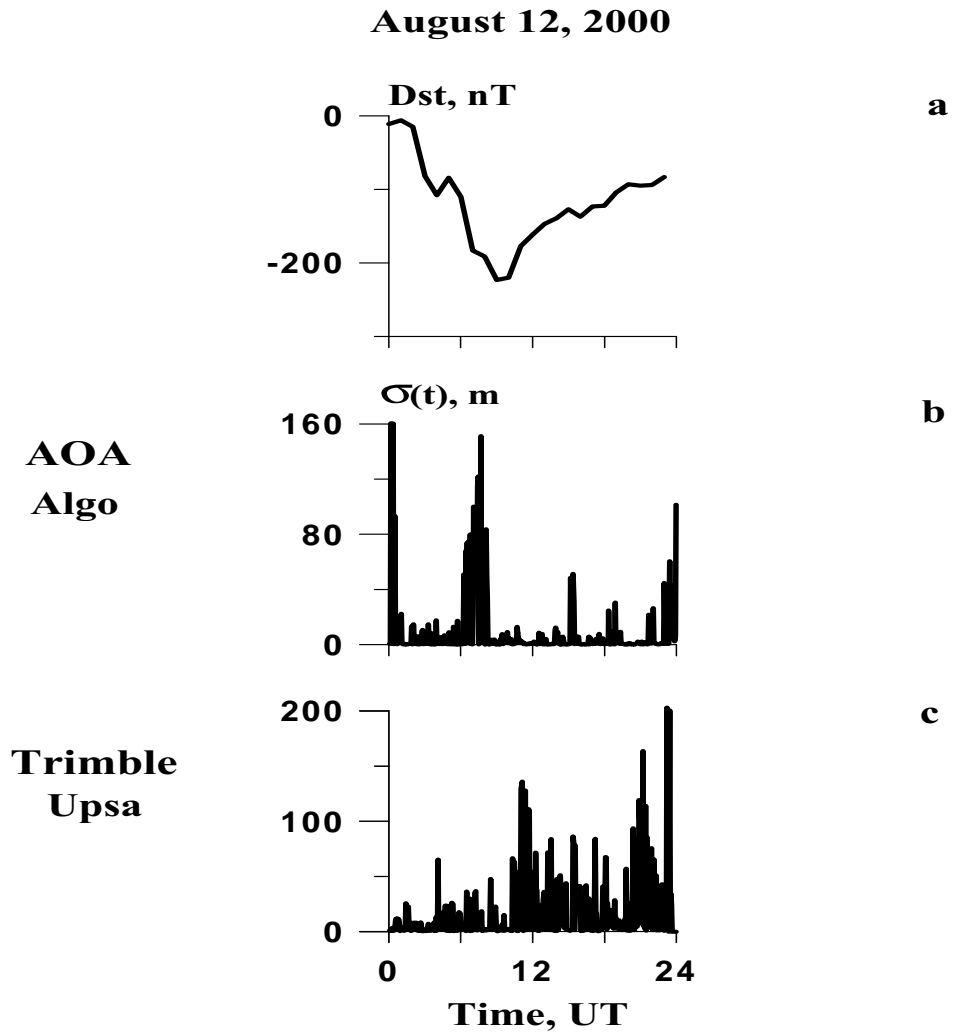


Figure 7: Diurnal variations of the magnetic disturbance index Dst for the magnetically disturbed day of August 12, 2000 - panel a). Diurnal variations of the standard deviation $\sigma(t)$, m in the location determination, inferred using the data from the AOA receiver installed at site Algo - b) and data from the Trimble receiver installed at site Upsa - c).

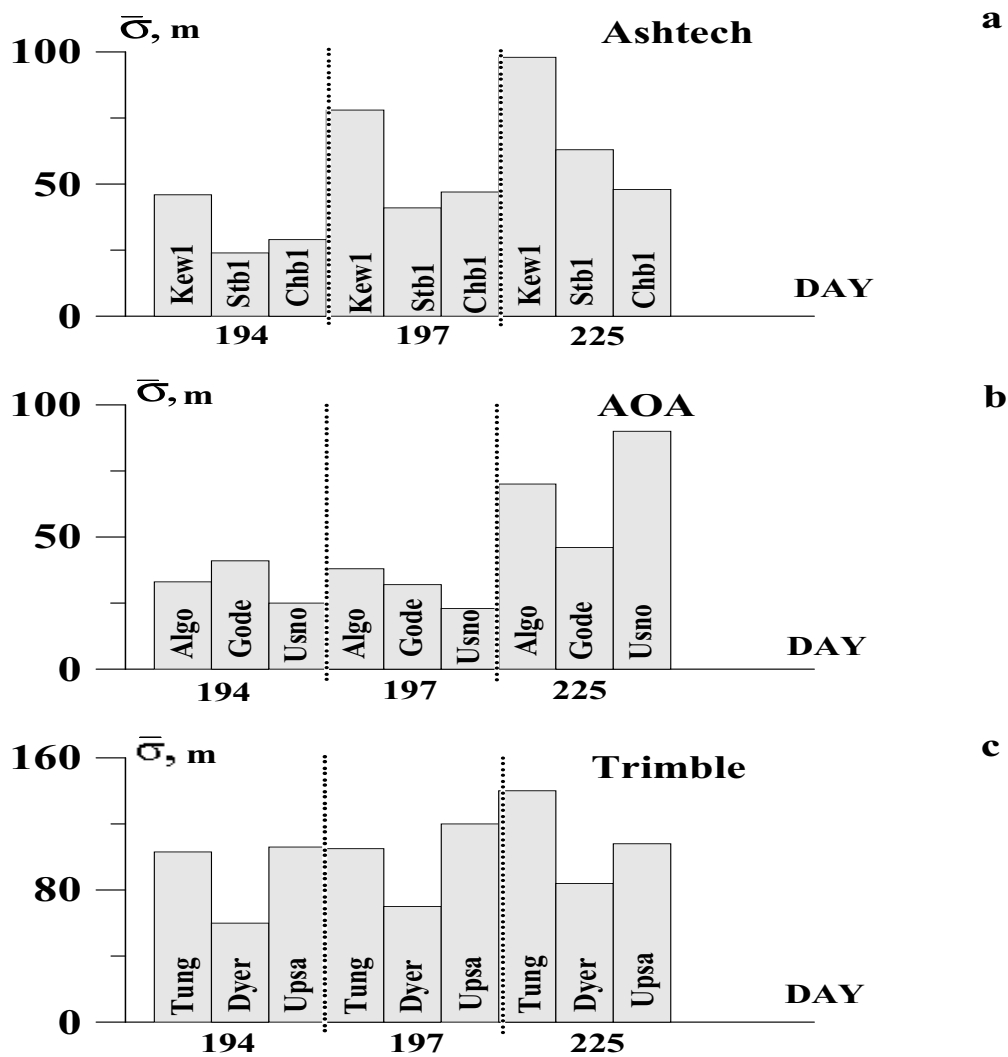


Figure 8: Distributions of daily mean standard deviations $\bar{\sigma}, m$ in the location determination for one magnetically quiet (194) and two magnetically disturbed (197 and 225) days of 2000, obtained at three sites for each of the three types of receivers: Ashtech - Kew1, Stb1 and Chb1 - (a), AOA - Algo, Gode and Usno - b), and Trimble - Tung, Dyer and Upsa - c).

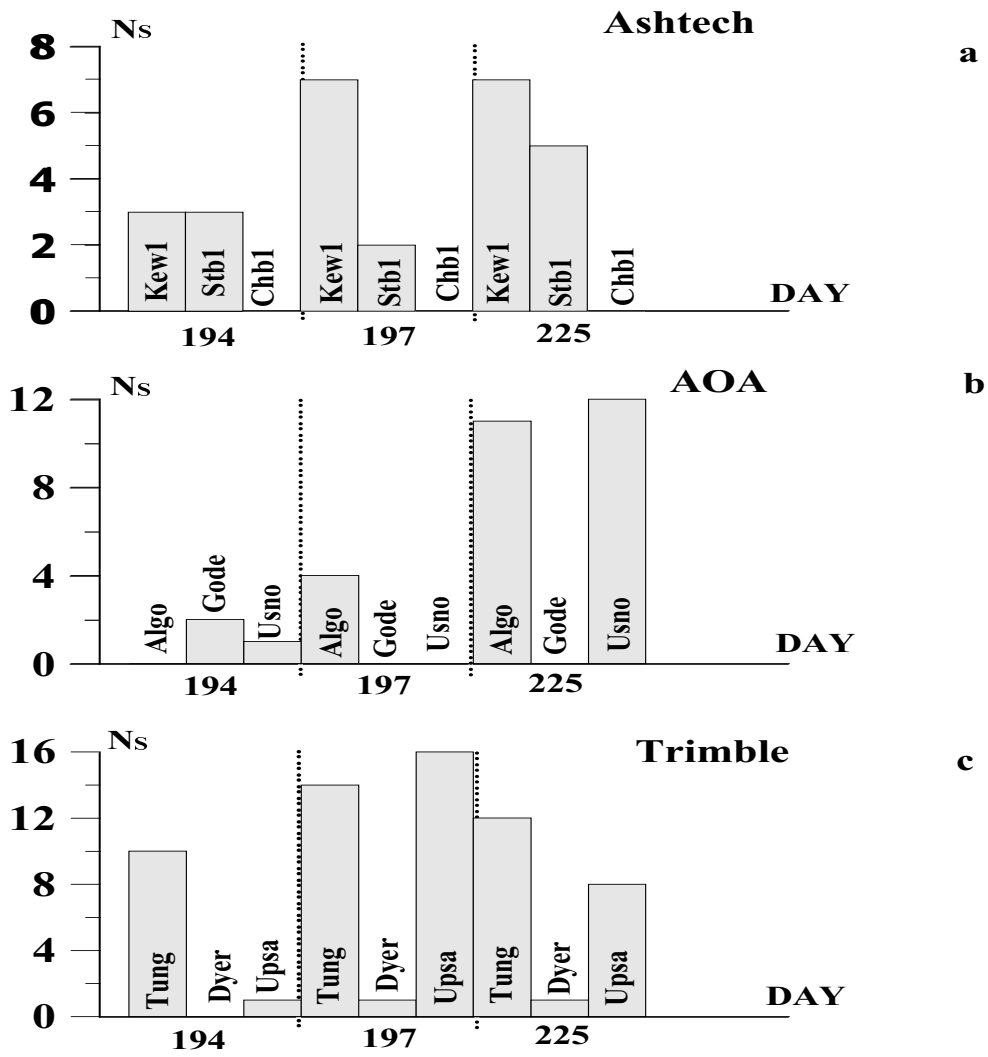


Figure 9: Distribution of the daily mean number of slips N_s in the location determination in the one-frequency mode, recorded at the sites with receivers of the following types: Ashtech - a), AOA - b), and Trimble - c).

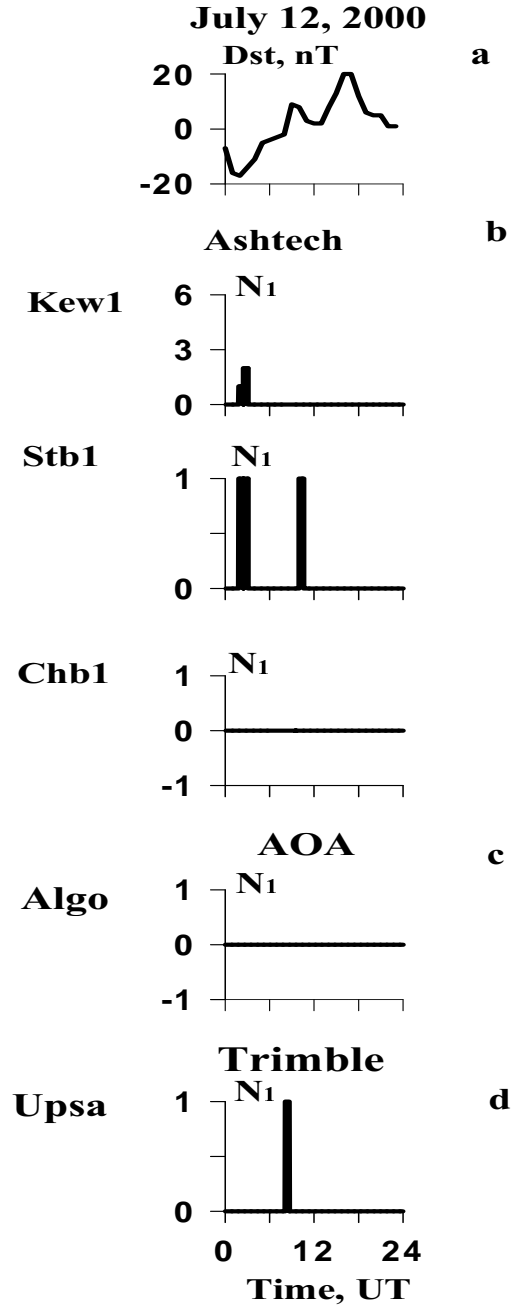


Figure 10: Diurnal variations of the magnetic disturbance index Dst for the magnetically quiet day of July 12, 2000 - panel a). Diurnal dependencies of the current density of slips N_1 of the one-frequency mode, recorded by the receivers: Ashtech (Kew1, Stb1 and Chb1) - panel b), AOA (Algo) - panel c), and Trimble (Upsa) - panel d).

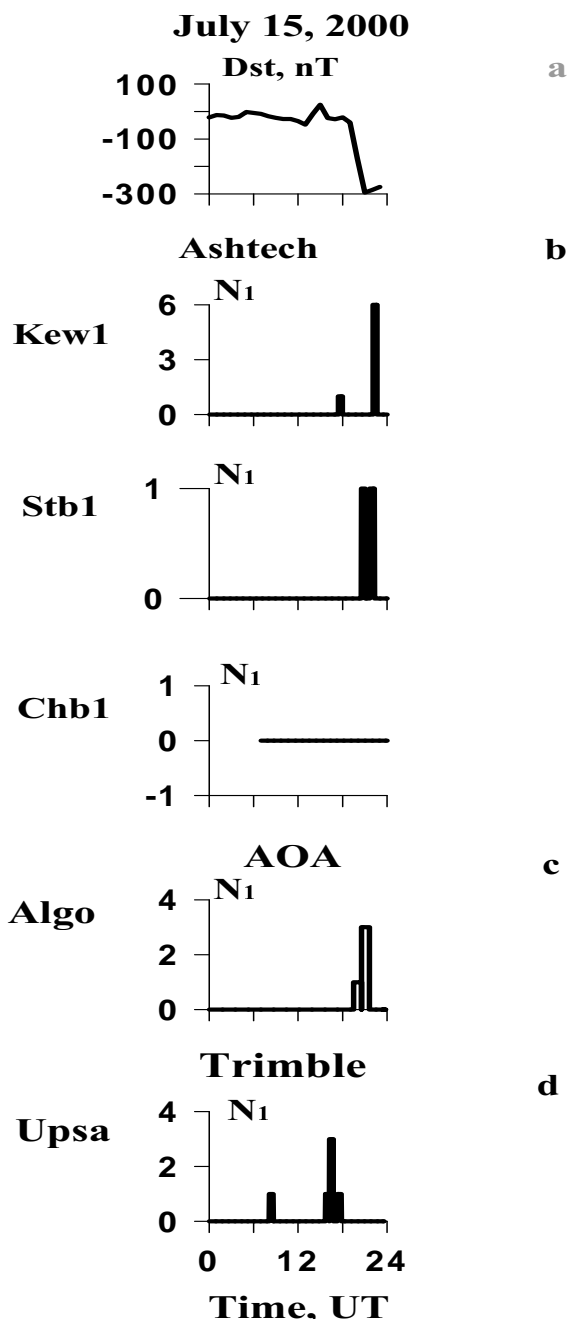


Figure 11: Diurnal variations of the magnetic disturbance index Dst for the magnetically disturbed day of July 15, 2000 - panel a). Diurnal dependencies of the current density of slips N_1 of the one-frequency mode, recorded by the receivers: Ashtech (Kew1, Stb1 and Chb1) - panel b), AOA (Algo) - panel c), and Trimble (Upsa) - panel d).

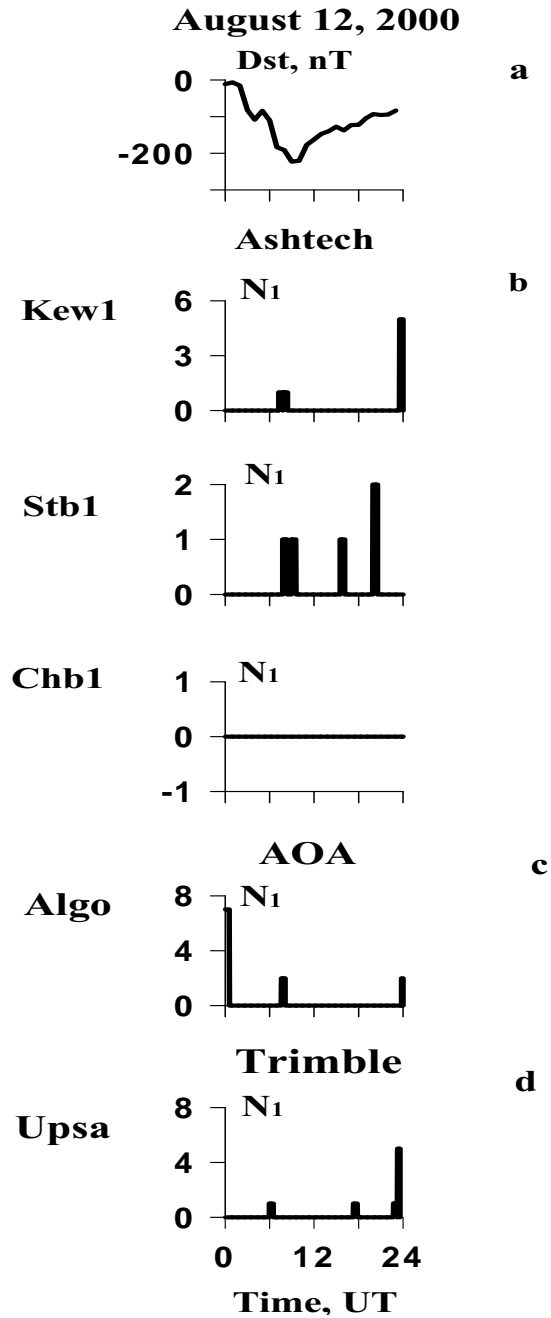


Figure 12: Diurnal variations of the magnetic disturbance index Dst for the magnetically disturbed day of August 12, 2000. Diurnal dependencies of the current density of slips N_1 of the one-frequency mode, recorded by the receivers: Ashtech (Kew1, Stb1 and Chb1) - panel b), AOA (Algo) - panel c), and Trimble (Upsa) - panel d).

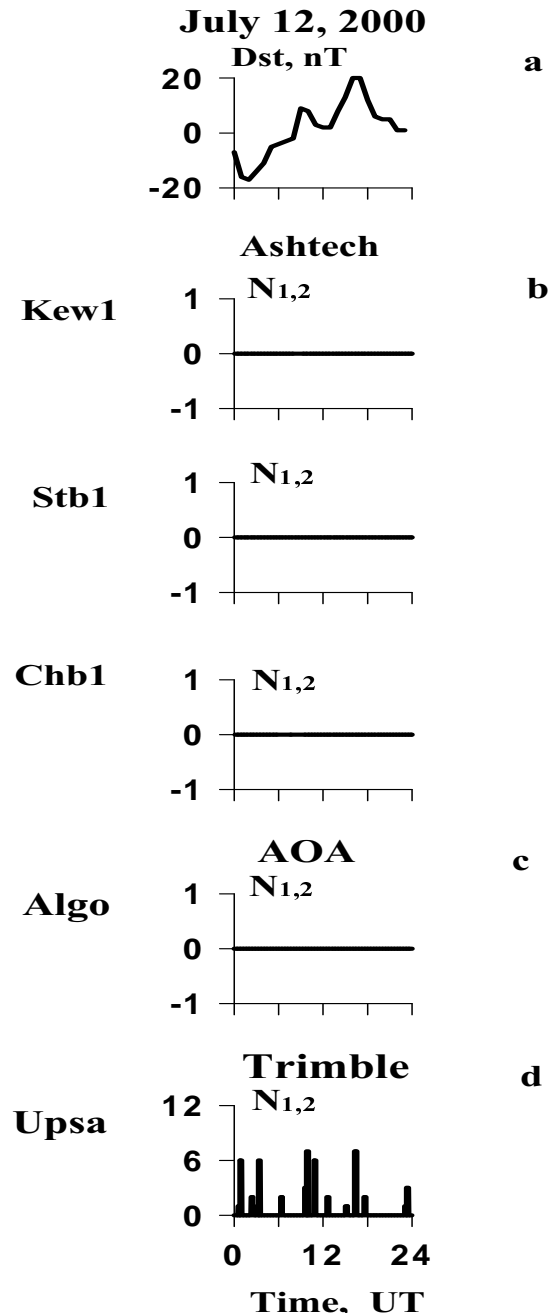


Figure 13: Diurnal variations of the magnetic disturbance index Dst for the magnetically quiet day of July 12, 2000 - panel a). Diurnal variations of the current density of slips $N_{1,2}$ of the two-frequency operating mode of the following receivers: Ashtech (Kew1, Stb1 and Chb1) - panel b); AOA (Algo) - panel c); Trimble (Upsa) - panel d).

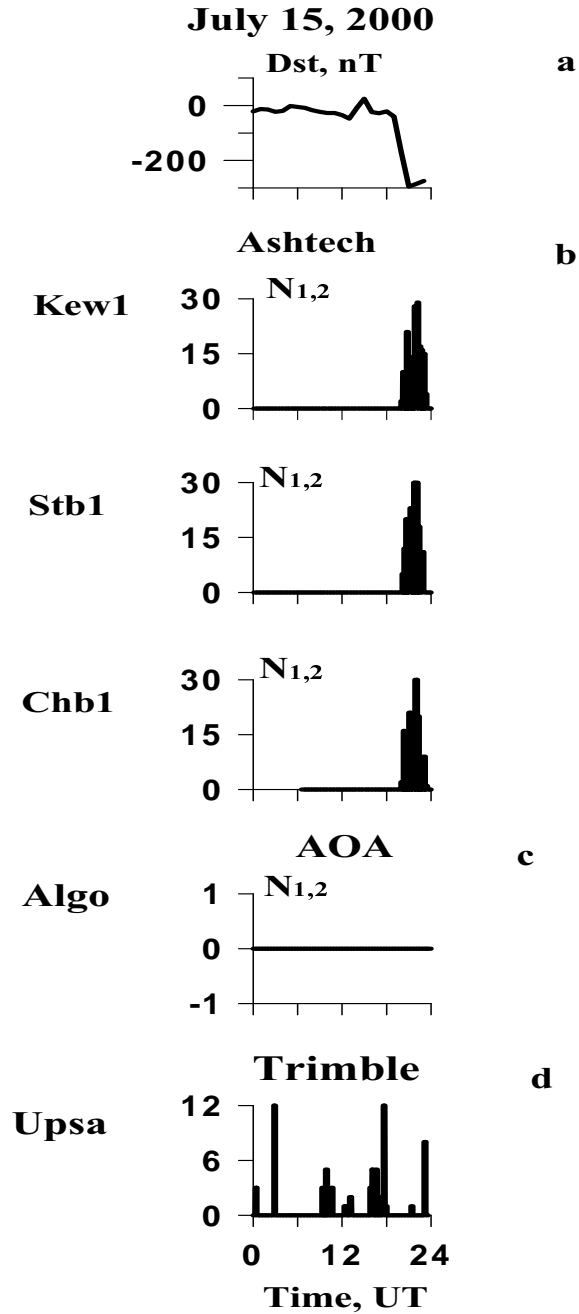


Figure 14: Diurnal variations of the magnetic disturbance index Dst for the magnetically disturbed day of July 15, 2000 - panel a). Diurnal variations of the current density of slips $N_{1,2}$ of the two-frequency operating mode of the following receivers: Ashtech (Kew1, Stb1 and Chb1) - panel b); AOA (Algo) - panel c); Trimble (Upsa) - panel d).

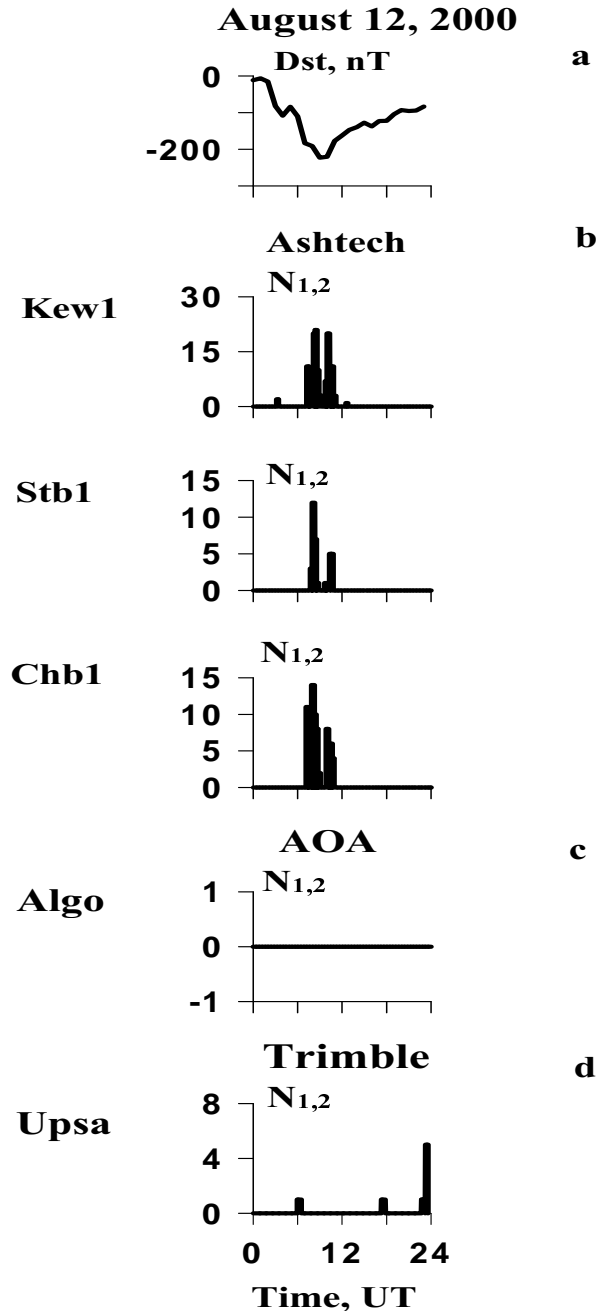


Figure 15: Diurnal variations of the magnetic disturbance index Dst for the magnetically disturbed day of August 12, 2000 - panel a). Diurnal variations of the current density of slips $N_{1,2}$ of the two-frequency operating mode of the following receivers: Ashtech (Kew1, Stb1 and Chb1) - panel b); AOA (Algo) - panel c); Trimble (Upsa) - panel d).

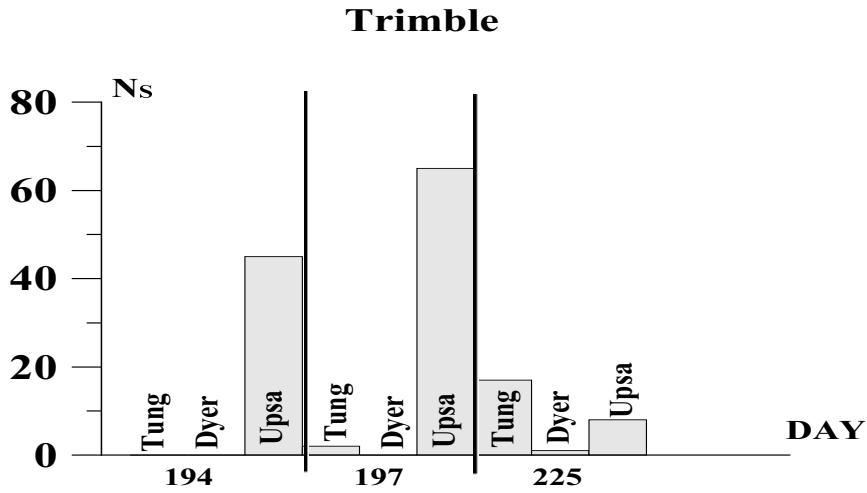
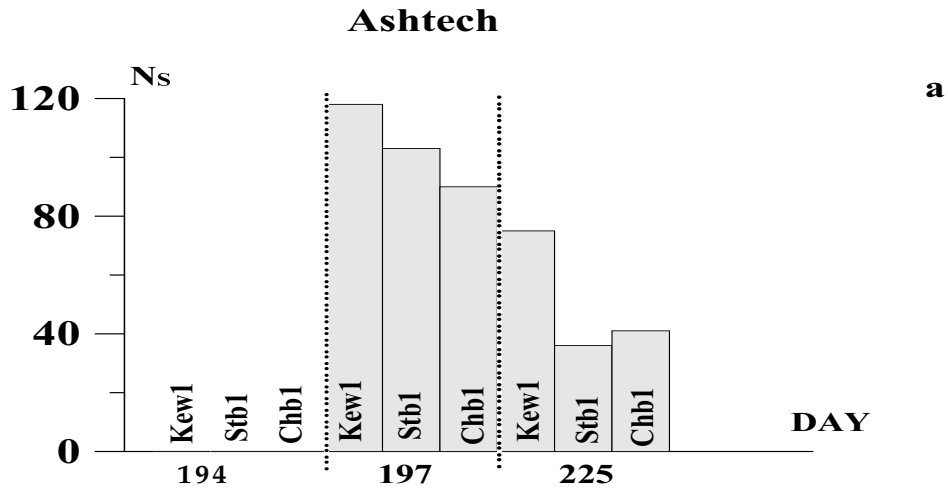


Figure 16: Distributions of the daily mean number of slips N_s of the two-frequency mode, recorded at the sites with Ashtech - a), and Trimble - b).

Table 1: Statistics of experiments

Date	Dst_{max} , nT	Station	Location (B, L deg.)	GPS receivers
12.07.2000 (194)	-17	Kew1	44.8; -87.3	Ashtech
		Stb1	45.7; -84.5	
		Chb1	47.2; -88.6	
		Algo	46; -78	AOA
		Gode	39; -76.8	
		Usno	38.9; -77	
		Tung	37.7; -118	Trimble
		Dyer	39.6; -118.8	
Upsa	40.4; -118.3			
15.07.2000 (197)	-295	the same		
12.08.2000 (225)	-223	the same		

Table 2: Data set of maxima rms of positioning error σ_{max}, m

GPS receivers	Station	Date of 2000		
		194 (July, 12)	197 (July, 15)	225 (August, 12)
		σ_{max}, m	σ_{max}, m	σ_{max}, m
Ashtech	Kew1	249	268	314
	Stb1	103	91	152
	Chb1	45	92	142
AOA	Algo	258	241	253
	Gode	190	125	114
	Usno	125	130	273
Trimble	Tung	243	231	361
	Dyer	110	314	337
	Upsa	174	242	327